

Mn-Zn ferrite line EMI suppressor for power switching noise in the impulse/high current bias regime

Dragana PETROVIĆ^{1,*}, Miroslav LAZIĆ¹, Obrad ALEKSIĆ²,
Maria Vesna NIKOLIĆ², Vedran IBRAHIMOVIĆ³, Milan PAJNIĆ¹

¹Iritel a.d. Beograd, Belgrade, Serbia

²Institute for Multidisciplinary Research, University of Belgrade, Belgrade, Serbia

³Military Technical Institute, Belgrade, Serbia

Received: 04.10.2017

Accepted/Published Online: 03.04.2018

Final Version: 28.09.2018

Abstract: Ferrite cores 50 mm long were formed from large ferrite tubes obtained using fine Mn-Zn ferrite powder (M-30-IHIS) extruded and sintered at 1280 °C for 2 h. Core impedance was measured in the HF range (0.1–100 MHz), varying the number of coil turns and DC bias. Characteristic parameters such as maximum of impedance Z_m , frequency of maximum impedance F_m , and suppressing range f around F_m were determined for each configuration. The analyzed ferrite cores were tested as round cable suppressors in the impulse regime. Impulses were generated by MOSFET transistor switching of high currents (1–10 A). The number of turns, impulse current, and DC bias current were varied in the range from 0 to 10 A. Magnetic interference configurations were formed on the ferrite core using opposite wound coils and tested in the impulse regime. Suppressor responses to different impulses were mutually compared and analyzed. Finally, two ferrite cores were EM coupled by a short circuited coil to form a novel line EMI suppressor aimed for suppression of power switching noise. Several configurations were formed with coupled cores acting on a magnetically interfering principle with opposite coils. The realized configurations were analyzed in view of application for EMI suppression in an uninterruptible power supply and AC/DC and DC/DC converters.

Key words: Mn-Zn ferrite, electromagnetic interference suppressors

1. Introduction

Electromagnetic interference (EMI) noise has increased significantly in the second part of the last century due to a huge rise in utilization of electronic equipment. First EMC regulations were developed and applied in different growing fields of electronics to overcome this problem, and this process has continued. The regulations moved engineers and researchers to invent and apply many different EMI suppressors to act in LF, MF, and HF ranges to prevent the deformation and interference of signals in electronic equipment and networks [1–6]. Generally, irradiated EMI noise is lowered by metal shielding, metal housing, and grounding of electronic equipment. Conductive EMI noise is suppressed on input and output terminations of electronic equipment using electronic components such as impulse arresters, varistors, and TVS diodes as the first input barrier; ferrite inductors as the second barrier; and capacitors combined with ferrite inductors as the third barrier [7, 8]. As electronic equipment varies, for example, from miniature small units (mobile phones) to networks (power networks, telecommunication networks, industry electronics) and from domestic appliances to medicine,

*Correspondence: titelac@iritel.com

military electronics, and many other fields of application, EMI suppressors differ in power, frequency range, insertion loss, construction, dimensions, and other characteristics [9–11].

EMI ferrite suppressors are produced worldwide and applied in electronics and telecommunications everywhere, e.g., from power sources such as AC and DC-DC converters to signal processing units [12–15]. Traditionally, both Mn-Zn and Ni-Zn ferrites and their combinations are used for EMI core production [16–18]. Fine powder grades and more recently nanostructured ferrites are used for EMI ferrite cores [19, 20]. The ferrite inductive effects on EMI suppression have been investigated and modeled for ferrite cores with different shapes and dimensions [21–23]. Beads and tubes are the most common EMI ferrite cores.

In our previous work [24, 25], we focused on constructing bundle EMI suppressors (groups of smaller tubes connected in series or in parallel) using different sized tubes and different configurations in view of possible applications in a wide frequency range (0–500 MHz), and this remains a work in progress. In this work we aim to design an EMI suppressor for a specific application: power switching noise in uninterruptible power supply (UPS) units, and thus in a specific MF frequency range (0.1–100 MHz).

Power switching EMI noise (generated by IGBTs, MOS transistors, and thyristors in high current switching AC/DC and DC/DC converters and UPS units) belongs to the MF range (0.1–10 MHz). Therefore, EMI suppressors for power switching noise in UPS units first need to suppress noise from the power network at 220 Vac/50 Hz: irradiated noise (unexpected) and conducted noise (unknown), and also self-switching noise generated in UPS converters [26, 27]. Generally, noises in UPS units are pulses (positive peaks) or interrupts (negative peaks). As the switching noise suppressor acts in the MF range (0.1–100 MHz), impedance in the EMI suppressor such as ωL and $1/\omega C$ requires large values of L and C . For inductors L the solution is to use larger ferrite cores and to choose ferrites with higher magnetic permeability (Mn-Zn ferrites instead of Ni-Zn ferrites), larger numbers of turns, and a suitable suppressing principle. Another problem in inductive suppressors with ferrites is a high DC bias current from the UPS unit with switching noise from the power network. To suppress the peaks we have to apply a self-impedance rise, magnetic interference, or magnetic coupling with opposite coils. Even impulses alone (with zero DC bias) are sometimes intensive enough to saturate ferrite cores.

The main idea in this work was to develop a line EMI switching noise suppressor for commercial UPS units in the 0.1–100 MHz range and in the impulse regime with DC bias (0–10 A). Mn-Zn ferrite was chosen as the magnetic material and a large custom-designed round cable ferrite core was produced with a large hole for a power cable conducting high currents. Impedance of the ferrite core was measured in the MF regime with DC bias while the number of turns was varied as a parameter. Then the same core was measured in the impulse regime also with DC bias. The aim was to optimize the working point and suppressing frequency range for a novel EMI suppressor with EM coupled cores with a short circuited coil between two cores.

2. Ferrite grade characterization

Commercial Mn-Zn ferrite powder (M-30 IHIS Ferrites, Belgrade, Serbia) was used. It was additionally milled for 12 h in slow ball mills to reduce grain size. Small disks and toroids were pressed and then sintered to 1280 °C for 2 h. They were used for ferrite grade characterization.

The relative magnetic permeability and dielectric permittivity were measured on an Agilent E5071B network analyzer using the method described in [28, 29]. The results obtained are given in Figure 1 and Figure 2.

Figure 1 shows that the magnetic properties do not change significantly up to 3 MHz. The real part

of magnetic permeability $\mu r'$ is close to 250 and $\mu r''$ is around 0 in the same frequency range. In the region from 10 to 100 MHz the real part has a gentle slope from 250 to 40 while the imaginary component increases to values near 120 at 25 MHz and decreases to close to 75 at 100 MHz, as shown in Figure 1. The imaginary component of relative magnetic permeability represents losses of the magnetic energy in the analyzed ferrite.

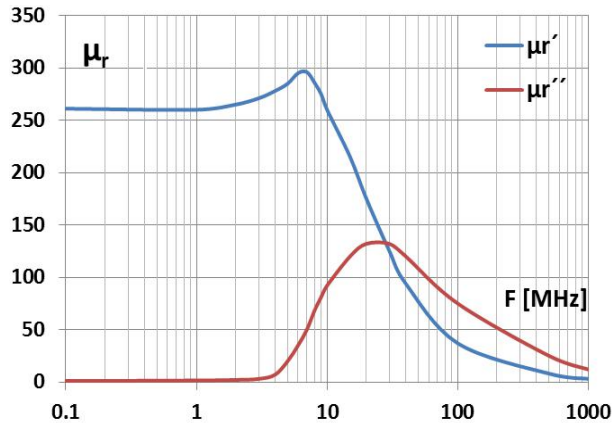


Figure 1. Relative magnetic permeability of Mn-Zn ferrite vs. frequency in the MF range: $\mu r = \mu r' + j\mu r''$ where, $\mu r'$ and $\mu r''$ are the real and imaginary components, respectively.

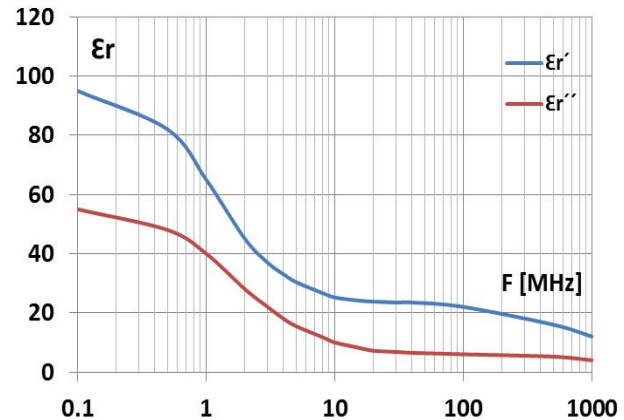


Figure 2. Relative dielectric permittivity of Mn-Zn ferrite vs. frequency in the MF range: $\epsilon r = \epsilon r' + j\epsilon r''$ where $\epsilon r'$ and $\epsilon r''$ are the real and imaginary components, respectively.

The dielectric permittivity is given in Figure 2. It decreases in the MF region also with a gentle slope where the real component $\epsilon r'$ decreases from close to 100 to 20, while $\epsilon r''$ decreases from close to 50 to 10. This is also suitable as at frequencies higher than 100 MHz the impedance Z decreases moderately in the capacitive region.

The hysteresis loop was measured on a hysteresis graph for soft ferrites LMM-1 (IHIS-Magnets, Belgrade, Serbia) using sintered toroid samples, at frequency $f = 10$ kHz, as shown in Figure 3.

The magnetic field (H) was increased by increasing the DC current (I) in the primary coil wound with $N_1 = 10$ turns on the toroid sample. H was calculated as $H = N_1 I / l_e$, where l_e is the effective circular length of the toroid (ring). The magnetic flux Φ was measured with a flux-meter probe (coil with $N_2 = 100$ turns) also wound on the toroid sample. Magnetic induction (J) was calculated from the flux as $J = \Phi / N_2 S$, where S is the cross-section area of the toroid.

The obtained hysteresis loop represents S-type hysteresis with gentle slopes and saturation $J > 0.45$ mT after $H > 100$ A/m. This is suitable for power current suppressors in UPS units as the analyzed ferrite core does not reach saturation at defined maximum currents such as 10 A, for example.

3. Round ferrite core in the MF regime

Custom-designed round cable ferrite cores, as shown in Figure 4, were made: outer diameter 20 mm, inner diameter 10 mm, and core length 50 mm. They were characterized in the MF regime (0.1–100 MHz) using an Agilent 8753 ES vector network analyzer. The schematic diagram and a photograph showing the measurement set-up are presented in Figure 5.

A measured round cable ferrite core wound with different numbers of turns and a ferrite core with an additional magnetizing coil with DC current bias are shown in Figure 6.

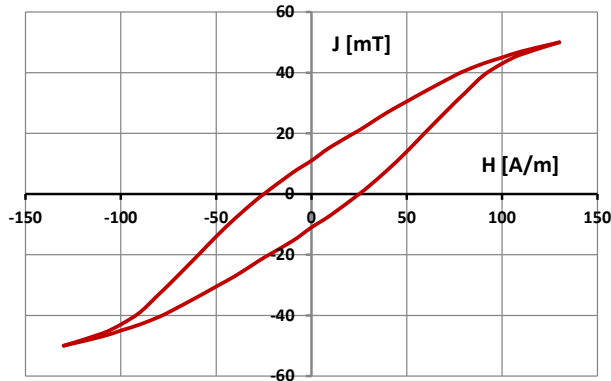


Figure 3. Hysteresis loop of sintered toroid samples produced of Mn-Zn ferrite (M-30-IHIS).



Figure 4. Custom-designed round cable ferrite core.

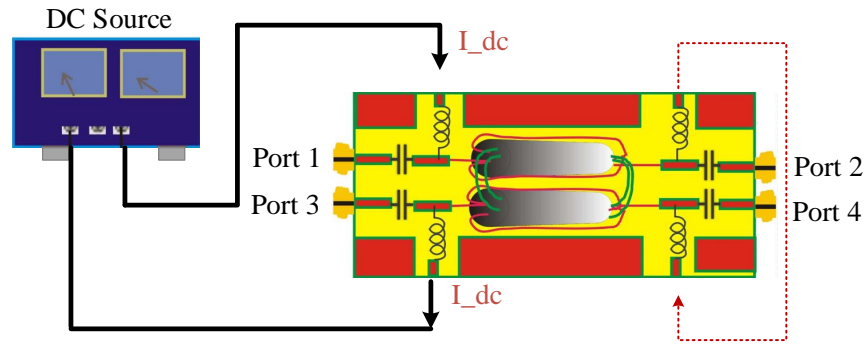


Figure 5. The schematic diagram measurement test: DC source, vector analyzer, and ferrite core.

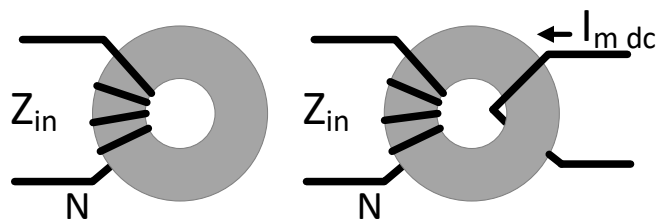


Figure 6. Round cable ferrite core wound with different numbers of turns (left) and ferrite core with an additional magnetizing coil (right) with DC current bias I_m (front view).

Characteristic parameters such as maximum of impedance Z_m at frequency F_m and in the suppressing range f around F_m (defined as $0.707 Z_m$) were calculated and are given in Table 1 and Table 2.

The input impedance was measured as a function of frequency while the number of turns (N) was varied as a parameter. The obtained impedance values are shown in Figure 7. Increasing the number of turns N from 1 to 10 leads to an increase of the maximum of impedance from around 1 to 20 k Ω , while the frequency of that maximum decreases from about 310 to 6 MHz, as given in Figure 7 and Table 1. The frequency of the

Table 1. Round cable ferrite core impedance vs. frequency (different numbers of turns).

N	Z_m [Ω]	F_m [MHz]	F_1 [MHz]	F_2 [MHz]	$f = F_2 - F_1$ [MHz]
1	988	308	44.61	404.1	359.5
2	2497	93	42.52	153.37	110.8
3	3918	50	27.92	78.01	50.08
4	5192	32	17.48	50.68	33.21
5	6489	19	11.51	29.37	17.86
6	8196	15	9.35	22.15	12.8
7	10,218	11	7.68	16.53	8.85
8	12,387	8.8	6.31	12.27	5.96
9	15,021	7.4	5.49	9.86	4.37
10	17,966	5.9	4.59	7.7	3.11

Table 2. Round cable ferrite core impedance vs. frequency (different currents).

I_m [A]	Z_m [Ω]	F_m [MHz]	F_1 [MHz]	F_2 [MHz]	$f = F_2 - F_1$ [MHz]
0	5902	31.2	18.93	45.57	26.64
3	5798	31.3	19.13	45.81	26.68
5	5756	31.4	19.86	46.32	26.46
8	5748	30.4	21.17	47.55	26.38
10	5734	30.5	22.81	48.57	25.76

suppressing range Δf around F_m defined at 0.707 of Z_m also decreases from 360 to 3 MHz as the number of turns increases.

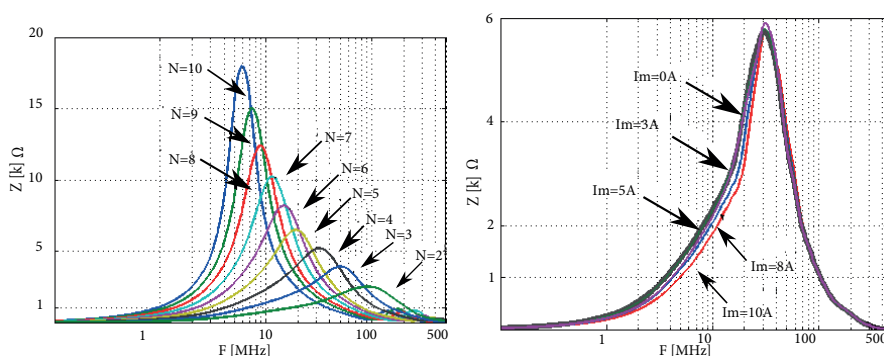


Figure 7. Impedance of a ferrite round cable core made of M-30 ferrite vs. frequency in the MF range. N - Number of turns (left). With DC current bias I_m - DC bias current (right).

Then $Z_{in} = Z$ was measured for the same core but for a fixed number of turns (in this case four, $N = 4$, as shown in Figure 6), and the core was externally magnetized with DC bias current I_m in the range of 0–10 A by an additional one pass of the wire through the hole of the ferrite core. The obtained impedance is shown on the right in Figure 7. When DC magnetizing current I_m is applied through an additional one pass of the wire through the hole of the ferrite core are given on the right in Figure 7 and in Table 2, the maximum of impedance Z_m (for $N = 4$ turns) is between 5.7 and 5.9 $k\Omega$, approximately. Increasing I_m from 1 to 10 A DC through the

additional coil decreases F_m from 31.2 to 30.5 MHz and also decreases the suppressing range from 26.6 to 25.8 MHz. The values in Table 2 and Figure 7 (right) are very close to real currents in UPS units although measuring signals and magnetizing current are magnetically superposed on the ferrite core with two separated coils while in practice noise and DC currents are in the same wire. The insertion loss in the small signal regime can be determined from impedance Z as $A = 20 \log(Z/50\omega)$. The impedance changes from around 2 to 6 $k\Omega$ from 10 to 50 MHz, giving an insertion loss from 32.4 to 40 dB. This is quite suitable for switching noise suppression in UPS and power supplies.

4. Round cable ferrite core in the impulse regime

The same round cable ferrite cores were tested in the impulse regime: first high currents were switched by a MOSFET transistor to form a stream of impulses V_{in} , as shown in Figure 8, while V_{out} and I were observed using a Tektronix TPS-212B digital storage oscilloscope and plotted versus time. The number of turns N was changed as a parameter. Impulses of 2 and 10 A were analyzed. The high currents switched by a MOSFET transistor were controlled by a function generator. The first (switch ON or step up) and the last (switch OFF or step down) edges were plotted on separate diagrams versus time: practically, the ferrite in the impulse regime core acts as a switching noise suppressor. Step up and step down edges of input current impulse are given in Figure 8. After that, the number of turns was fixed to $N = 4$ and the core was externally magnetized with DC bias current I_m in the range of 0–10 A using an additional one pass of the wire through the hole of the ferrite core. Impulses of 2 and 5 A were analyzed.

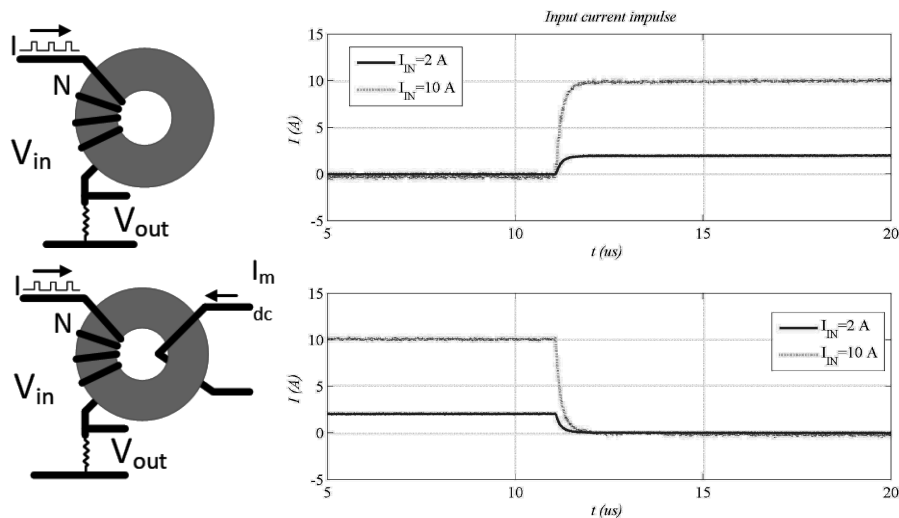


Figure 8. Round cable ferrite core in the impulse regime: varying N number of turns (top), I_m - magnetizing DC bias current varied for 4 turns (bottom), step up and step down edges of input current impulse (right).

The responses of the ferrite core as a suppressor to the “step up” part of the impulse for two switching current values of 2 A and 10 A as shown in Figure 9 show an increase of delay of the “first edge” with increasing number of turns. The delay is higher for higher switching steps of 10 A compared to 2 A. This can be explained by a rise of impedance and growth of relative magnetic permeability on the hysteresis loop with increasing magnetic excitation force. The “step down” responses shown in Figure 9 present the “tail effect” or a delay effect that also increases with the number of turns as $Z(N)$ increases. The delay is longer for higher step down inputs of 10 A compared to 2 A, as given in Figure 9.

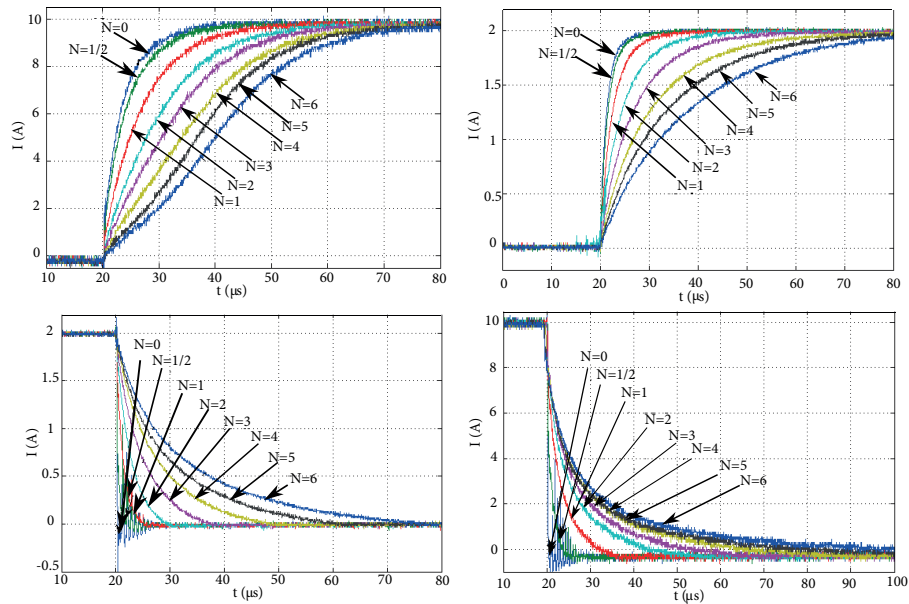


Figure 9. Response of a round cable ferrite suppressor to step up and step down input current: $I = 2$ A (left), $I = 10$ A (right), N number of turns varied as a parameter. $N = 0$ without a ferrite core.

The suppressor responses to step up and step down switched currents of $I = 2$ A and 5 A and DC bias current variations (0–10 A) are given in Figure 10, respectively.

It can be noticed that the DC bias and the switching current are superposed magnetically on the same core and together simulate load changes in the UPS unit and switch on and switch off regime.

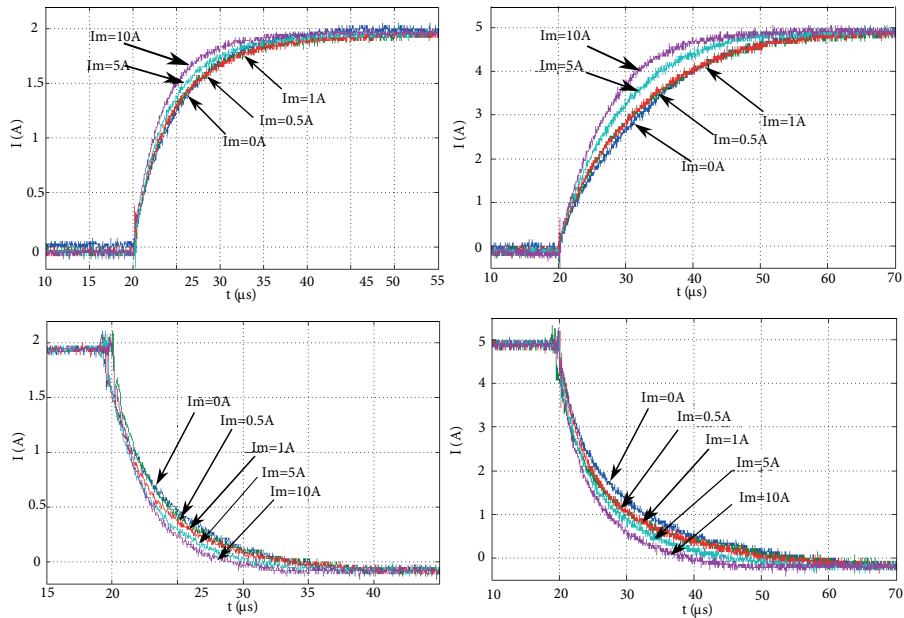


Figure 10. Response of a round cable ferrite suppressor to step up and step down input current: $I = 2$ A (left), $I = 5$ A (right), number of turns $N = 4$, and DC bias current varied as a parameter. $N_2 = 1$.

The responses to step up and step down current inputs with additional DC current bias I_m are given in Figure 10, showing different effects compared to when there is no current bias, $I_m = 0$, as given in Figure 9. The switching currents are superposed magnetically with the DC bias I_m magnetizing current. When the knee of ferrite magnetic saturation is reached permeability decreases a little with $(NI + N_b I_m)$ increase (N_b - bias current turns). Impedance Z also decreases a little with I and N increasing. Fortunately, at 10 A, DC currents passing through the round cable ferrite core do not cause ferrite magnetic saturation (the working point is below the knee of the hysteresis loop). Thus, the shapes of responses presented above are not deformed much and these working points can be used for efficient impulse suppression in UPS units during occasional stunning changes of load power from 0 to 2 kW, or even more.

5. Round cable ferrite core and magnetic interference principle

Two opposite wound coils with one or more turns on the same ferrite core can be used as an impulse self-interfering device: the main current is divided into two halves and the opposite wound coils are magnetically coupled by the ferrite core. Then the produced magnetic fluxes are in opposite directions so the noise impulses have interference. Two ferrite cores can also be joined into one magnetic device by coupling a short circuited coil between them. This way, a dual core is formed like a very large “balloon” core, not as a single core but as an EM coupled core, representing a new magnetic device. Different configurations for interfering noise impulses can be formed and some examples are shown in Figure 11. The number of turns of opposite coils is $N = 4$.

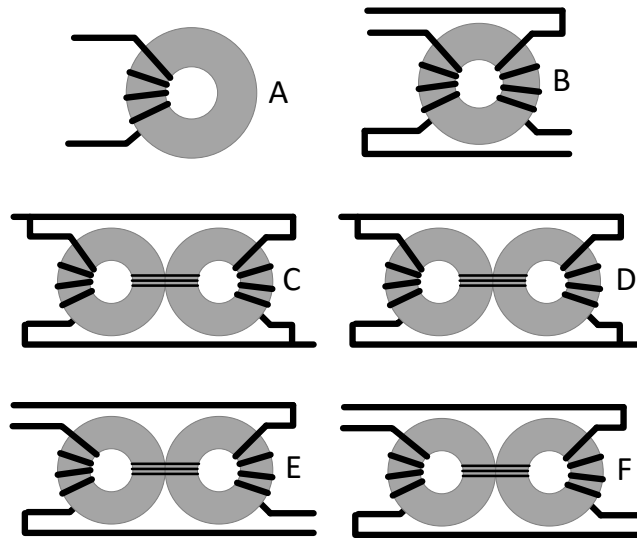


Figure 11. The magnetic interference principle and different configurations with one or two ferrite cores. Configurations with two ferrite cores are EM coupled by a short circuited coil.

The responses of different configurations in the impulse regime for impulses of 2 A are given in Figure 12 for step up and step down, e.g., the first and the second edge, respectively. The number of windings was fixed to $N = 4$.

The impulse responses depend on the suppressing principle used and the coil configuration on the ferrite cores. Configuration A, as shown in Figure 11, has only one coil and the response to step down and step up inputs is exponential, while configuration B, as shown in Figure 11, has self-magnetic interference with two opposite coils, which is very often used in impulse suppressors. The interference principle was tested with $N =$

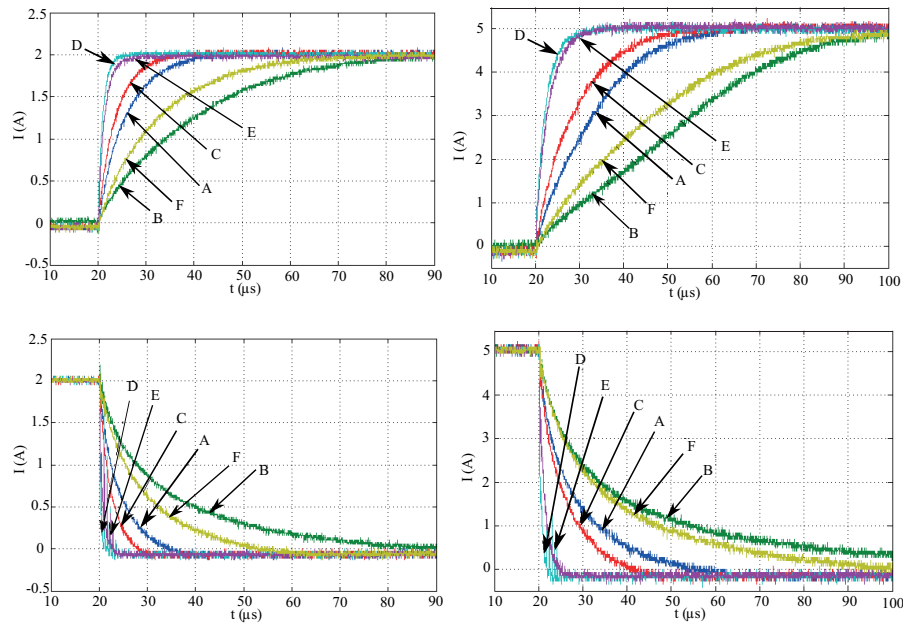


Figure 12. Impulse response to step up and step down function ($I = 2$ A (left) and 5 A (right)) for different configurations and fixed number $N = 4$ of windings.

4 turns on a single ferrite core. The effect of lowering the slope of the first edge (delay) for the step up input or tail forming for the step down input was double for the B configuration compared to the A configuration (with one coil).

Other configurations were formed with two cores EM coupled with 10 turns, as shown in Figure 11. In the case of configurations C and D the main current is divided into two halves passing through coils wound in the same and opposite directions, respectively. Configuration D superposes magnetic fluxes from both cores in the coupling short circuited coil without interfering, while configuration C interferes with magnetic fluxes and significantly changes the first edge and tail of the response. The delay effect is slightly smaller for configuration C compared to B as the current is lower (half of the main current). Configurations E and F are similar to inductive line filters by coil positions. In this case, the magnetizing effects are higher as the current is not divided into two halves. The forward and back current (like a phase and null) pass through different coils on different cores and magnetic fluxes have interference in the coupling coil for configuration F. In the case of configuration E, magnetic fluxes are superposed (not interfered with) and the effect on the first edge of the response is negligible. The effect on the first edge (delay) of the responses, as shown in Figure 12, is higher for higher currents (for 2 A and 5 A, respectively). Configuration F has a slightly smaller effect on the first edge and tail of the response than configuration B. However, there is more room to put conductors with a larger cross-section in configuration F, decreasing the number of turns and allowing much higher currents to pass through the ferrite core like a higher power switching noise suppressor. In practice, sometimes high intensity switching noise is a part of much higher AC and DC input currents.

The main intention of this work was to use an inductive suppressor on cables without large capacitors and to define experimentally the application limits and switching noise suppression efficiency in the MF range (0.1–100 MHz). The analyzed round cable ferrite core can be used as a single core suppressor or dual core switching noise suppressor for a switching noise suppressor in UPS units, as shown in Figure 7, Figure 8, and

Figure 11. Configurations A and B with a single ferrite core and E and F with dual cores can be applied as efficient switching noise suppressors.

6. Conclusion

A switching noise EMI suppressor with a Mn-Zn round cable ferrite core was formed and tested in the impulse/high current bias regime to determine the limits in applications such as input noise suppressors in UPS units and AC/DC and DC/DC converters. The obtained results have shown that in the MF frequency range (0.1–100 MHz) the round cable ferrite core changes properties in accordance with the decrease of magnetic permeability and dielectric permittivity of the ferrite with frequency and in accordance with variable noise switching current (impulse) intensity and steady bias current intensity (magnetizing current). The shape and size of the core and number of windings also play an important role in inductivity, working point on the hysteresis loop, and parasitic capacitance between the windings (turns). Optimum impedance Z and the operating principle of suppression were tested and analyzed. A single core and dual EM coupled cores with the interfering principle showed the best switching noise suppression in the impulse/high current regime.

Although a pure inductive solution for switching noise suppressors was chosen (without an electrolyte and ceramic capacitors), it showed relatively high suppression in the MF range. High reliability was demonstrated when it was exposed to high currents and impulses, e.g., switch on and off regime. These solutions can allow a large thermal dissipation due to the Joule effect in the ferrite. Thus, pure inductive line filters based on a dual core (configurations E and F, EM coupled as presented in this work) can be successfully used on cables connected to UPS units for suppressing high power switching noise generated in the power network.

References

- [1] Damnjanovic M, Stojanovic G, Živanov L, Desnica V. Comparison of different structures of ferrite EMI suppressors. *Microelectronics* 2006; 23: 42-48.
- [2] Cochrane D, Chen DY, Boroyevic D. Passive cancellation of common-mode noise in power electronic circuits. *IEEE T Power Electr* 2003; 18: 756-763.
- [3] Li H, Li Z, Zhang B, Tang WKS, Halang WA. Suppressing electromagnetic interference in direct current converters. *IEEE Circ Syst Mag* 2009; 9: 10-28.
- [4] Kincaid JE, McGregor MA. Electrical noise considerations in facility/plant design. *ISA T* 1993; 32: 291-296.
- [5] Bina MT, Pashajavid E. An efficient procedure to design passive LCL-filters for active power filters. *Electr Pow Syst Res* 2009; 79: 606-614.
- [6] Akagi H, Hasegawa H, Doumoto T. Design and performance of a passive EMI filter for use with a voltage-source PWM inverter having sinusoidal output voltage and zero common-mode voltage. *IEEE T Power Electr* 2004; 19: 1069-1076.
- [7] Foster J. Breakover diodes for transient suppression. *Electron Eng* 1987; 59: 35-39.
- [8] Yodogawa M. Zinc Oxide. Varistors provide urgent surge control. *Journal of Electrical Engineering* 1987; 24: 76-81.
- [9] Scott J, Van Zyl C. *Introduction to EMC*. Oxford, UK: Butterworth-Heinemann, 1997.
- [10] Weston DA. *Electromagnetic Compatibility: Principles and Applications*. New York, NY, USA: Marcel Dekker, 1991.
- [11] Tihanyi L. *Electromagnetic Compatibility in Power Electronics*. New York, NY, USA: IEEE Press, 1995.
- [12] Zhang R, Wu X, Wang T. Analysis of common mode EMI for three-phase voltage source converters. *IEEE Power Electron* 2003; 4: 1510-1515.

- [13] Li H, Li Z, Zhang B, Tang WKS, Halang WA. Suppressing electromagnetic interference in direct current converters. *IEEE Circ Syst Mag* 2009; 9: 10-28.
- [14] Mainali K, Oruganti R. Conducted EMI mitigation techniques for switch-mode power converters. *IEEE T Power Electr* 2010; 25: 2344-2356.
- [15] Li H, Li Z, Halang WA, Zhang B, Chen G. Analyzing chaotic spectra of DC-DC converters using the Prony method. *IEEE T Circuits-II* 2007; 54: 61-65.
- [16] Snelling EC. *Soft Ferrites: Properties and Applications*. 2nd ed. New York, NY, USA: Butterworths-Heinemann, 1988.
- [17] Goldman A. *Ferrites for EMI Suppression in Modern Ferrite Technology*. 2nd ed. Berlin, Germany: Springer, 2006.
- [18] Ott G, Wrba J, Lucke R. Recent developments of Mn-Zn ferrites for high permeability applications. *J Magn Magn Mater* 2003; 254-255: 535-537.
- [19] Shen W, Wang F, Boroyevich D, Tipton CW. Loss characterization and calculation of nanocrystalline cores for high frequency magnetics applications. *IEEE T Power Electr* 2008; 23: 475-484.
- [20] Fiorillo F, Beatrice C, Cołsson M, Zhemchuzhna L. Loss and permeability dependence on temperature in soft ferrites. *IEEE T Magn* 2009; 45: 4242-4245.
- [21] Saotome H, Sakaki Y. Complex permeability of polycrystalline Mn-Zn and Ni-Zn ferrites. *Electr Eng Jpn* 1998; 123: 1-7.
- [22] Yu Q, Holmes TW, Naishadham K. RF equivalent circuit modeling of ferrite-core inductors and characterization of core materials. *IEEE T Electromagn C* 2002; 44: 258-262.
- [23] Urabe J, Fujii K, Dowaki Y, Jito Y, Matsumoto Y, Sugiura A. A method for measuring the characteristics of an EMI suppression ferrite core. *IEEE T Electromagn C* 2006; 48: 774-780.
- [24] Blaz NV, Lukovic MD, Nikolic MV, Aleksic OS, Zivanov LjD, Lukic LS. Analysis of a Mn-Zn ferrite bundle EMI suppressor using different suppressing principles and configurations. *IEEE T Magn* 2013; 49: 4851-4857.
- [25] Blaz NV, Lukovic MD, Nikolic MV, Aleksic OS, Zivanov LjD. Heterotube Mn-Zn ferrite bundle EMI suppressor with different magnetic coupling configurations. *IEEE T Magn* 2014; 50: 800-907.
- [26] Kwasniok PJ, Bui MD, Kozłowski AJ, Stanislaw SS. Technique for measurement of powerline impedances in the frequency range from 500 kHz to 500 MHz. *IEEE T Electromagn C* 1993; 35: 87-90.
- [27] See KY, Deng J. Measurement of noise source impedance of SMPS using a two probes approach. *IEEE T Power Electr* 2004; 19: 862-868.
- [28] Lukovic MD, Nikolic MV, Blaz N, Zivanov LjD, Aleksic OS, Lukic LS. Mn-Zn ferrite round cable EMI suppressor with deep grooves and a secondary short circuit for different frequency ranges. *IEEE Tr Magn* 2013; 49: 1172-1177.
- [29] Blaz N, Maric A, Radosavljevic G, Zivanov L, Stojanovic G. Modeling and characterization of frequency and temperature variation of complex permeability of ferrite LTCC material. *Prog Electromagn Res B* 2010; 23: 131-146.